CORTEA PROJECT: DESOx NEW GEN

NON-CONFIDENTIAL SYNTHESIS

Activity period: September 2012 - March 2015

Project carried out by (GE, CNRS, UHA) – Contract N° 1281C0039, 1281C0083, 1281C0084

Details of the coordinating body:

GE EPF - Matthieu Vierling - Product Engineering Department – 20 avenue du Maréchal Juin - BP379 - 90007 Belfort Cedex

GE EPF – Michel Molière (until 31/12/2013)

Details of the partner laboratories:

Institute of Materials Science of Mulhouse (IS2M), Materials with Controlled Porosity Team (MPC) - Pierrick Gaudin, Joël Patarin, Habiba Nouali – UMR CNRS 7361 University of Haute Alsace, 3 b rue Alfred Werner - 68093 Mulhouse Cedex

Risk and Environment Management Laboratory (GRE) – Sophie Dorge, Jean-François Brilhac – University of Haute Alsace, 3 b rue Alfred Werner - 68093 Mulhouse Cedex

Technical coordination:

ADEME - Direction of Productions and Sustainable Energies - Emmanuel Fiani - Enterprise Service and Eco-Technologies – 20 avenue du Grésillé – BP 90406 – 49004 Angers Cedex 01 - France

ADEME
Agence de l'Environnement
et de la Maîtrise de l'Energie

In partnership with:

NON-CONFIDENTIAL SYNTHESIS

Acknowledgments

1. Introduction

Sulfur dioxide, a by-product of the combustion of fossil fuels and of numerous industrial processes, has adverse effects on health (affections asthmatic diseases, respiratory disorders, etc.) and contributes to the formation of atmospheric particles. Sulfur dioxide is also responsible for acid rain, which may damage crops, forests, and the ecosystem as a whole. Therefore, even if today the issue of acid rain has virtually been resolved, the impact of SO_2 emissions on ambient particulate matter means that reduction efforts are still necessary (see the commitments made under the amendments to the Göteborg Protocol, adopted in 2012).

Main sources of SO_2 emissions are coal-fired power plants, oil refineries, and natural gas and mineral processing plants. It should be noted that sulfur oxide emissions from large combustion installations (boilers, gas turbines, diesel engines, etc.) are governed by national and European regulations that will in the coming years be substantially tightened as a result of the ongoing development of BREFs (Best Available Techniques Reference Documents). Today these BREFs point to the drawbacks of conventional desulfurization techniques based on lime injection and stress the fact that the dry method uses much adsorbent and requires the management of large quantities of solid residues.

Today there are many cases where desulfurization at the source of the fuel is not industrially possible (by-products of processes, fermentation products of organic matter, domestic waste incineration plants). It is therefore desirable to have a post-combustion desulfurization process that is both economically viable and low energy efficient: reversible capture using a regenerative adsorbent appears to be a promising approach in this respect.

A bibliographical review (1) has enabled us to identify the main adsorbents currently used to capture SO_2. These are mostly non-regenerative adsorbents whose use on an industrial scale appears difficult to achieve.

This bibliographical study has also enabled us to identify the main physicochemical properties required to develop an efficient adsorbent for sustainable use on an industrial scale, notably:

- large specific surface area (at least greater than 600 $m^2.g^{-1}$),
- excellent thermal stability (at least up to 800°C),
- possibility of incorporating heteroelements required for the chemisorption of SO_X at high temperature,
- excellent inertness of the support to SOx,
- high regenerability potential during multi-cycle tests.

For this study, we have therefore chosen to use mesoporous silica materials as support. These materials have the advantages of large specific surface area (several hundreds of $m^2.g^{-1}$), high thermal stability (some up to 1000°C), good regeneration capacity, and allowing heteroelements to be incorporated into their porosity for the capture of SO_2 by chemisorption in the form of metal sulfate.

The adsorbent must be capable of operating in the presence of a gaseous feed consisting of 250 ppm of SO_2, 5 vol. % of water vapor, 10 vol. % of oxygen, the remainder being nitrous oxide, at a Gas Hourly Space Velocity (GHSV) of 25000 h^{-1} and a temperature of 400°C. The strategy to achieve this consists of impregnating the mesoporous silica supports with metal oxides so as obtain bifunctional

3

materials capable of catalyzing the oxidation of SO_2 to SO_3 (equation 1), chemisorbing the SO_3 in the form of sulfates (equation 2) and of being regenerated (equation 3).

Equation 1: $\quad\quad SO_2 + \frac{1}{2}\,O_2 \rightarrow SO_3$

Equation 2: $\quad\quad x\,SO_3 + MO_x \rightarrow M(SO_4)_x$

Equation 3: $\quad\quad M(SO_4)_x \rightarrow x\,SO_3 + MO_x$

2. Materials and methodology

This report presents the most significant results of the DeSOx New Gen program covering the period of activity from March 2013 to March 2015. The objective of this program is to develop a sulfur oxide (SO_X) adsorbent characterized by a high SOx adsorption capacity and possessing regenerability during multi-cycle tests. The strategy consists of modifying the mesoporous silica supports with oxides of heteroelements (Cu, Ce, Fe) capable of chemisorbing the SO_X in the form of sulfates.

In a first stage, the task consisted of choosing the most appropriate support to be used for this study. The experimental comparison of different mesoporous supports (MCM-41, KIT-6, SBA-15) shows that the SBA-15 ordered mesoporous silica support possesses better thermal stability than its homolog MCM-41, its synthesis is easier and more reproducible than its equivalent KIT-6, while at the same time has a pore size (5 to 10 nm) that promotes the diffusion of the gaseous species (SO_X) to be treated.

In a second stage, different heteroelements were impregnated alone (Cu, Fe, Zn, Ce) or in combination (Cu-Zn, Cu-Fe, Cu-Ce). To this end, several heteroelement impregnation methods were applied:

-   wet impregnation in water or methanol
-   incipient wetness impregnation
-   ion exchange
-   solid-solid grinding.

Special attention has also been paid to the drying and calcination conditions. Drying was carried out in an oven at different temperatures (from 25°C to 90°C) and by lyophilization. Two calcination temperatures (500°C and 700°C) were investigated. Calcination was carried out in a muffle furnace, using either a temperature ramp up or flash calcination (by placing the sample in a preheated furnace at 500°C), and in a tubular reactor under high synthetic air flow conditions.

4

3. Results and discussion

The overall results show that CuO/SBA-15 type adsorbents appear to be promising. It was demonstrated that different copper-based species are likely to exist: either nanometric or micrometric crystallized copper oxide (CuO) particles, or highly dispersed copper-based species strongly interacting with the support (Cu-O-Si).

For the purpose of correlating the efficiency of the adsorbents with their physicochemical properties, part of the work consisted of studying the impact of the dispersion and the nature of the copper on the efficiency of the adsorbents for the desulfurization reaction. For this study, impregnation by solid-solid grinding was preferred. In fact, impregnation by solid-solid grinding is reported to allow highly dispersed copper-based species (Cu-O-Si) (2; 3) strongly interacting with the support, to be obtained. Numerous tests were carried out, during which parameters such as the copper precursor and the drying and calcination conditions were varied. The acquired know-how allowed us to show that it is possible to control the nature of the deposited copper species by adjusting the calcination conditions:

- calcination with temperature ramp, under air flow in a muffle furnace for 6 hours at 500°C with a temperature ramp of 1°C/min. The material obtained, green colored probably due to formation of Cu-O-Si species, is called Cu/SBA-r-500 where "Cu" designates the copper, "SBA" the SBA-15 ordered mesoporous silica, "r" the calcination ramp, and "500" the calcination temperature.
- "flash calcination": the sample is placed in a preheated muffle furnace at 500°C and calcined under air flow for 6 h at 500°C. The material obtained, brown colored probably due to the formation of CuO particles, is called Cu/SBA-f-500, where "f" designates the flash calcination.
- calcination of the sample under air flow in a muffle furnace for 6 h at 700°C with a temperature ramp of 1°C/min. The material obtained, also brown colored, is called Cu/SBA-r-700.

The three materials have CuO contents between 10 and 12.5 wt. %. The XRD patterns at low angles and the nitrous oxide physisorption isotherms confirm that the mesoporous structure is preserved after incorporation of the copper. For the Cu/SBA-r-500 material, the XRD pattern shown in Figure 1 indicates the absence of peaks corresponding to the copper oxide, which suggests the formation of highly dispersed copper-based species strongly interacting with the support (Cu-O-Si) (4; 5; 6; 7; 8). This result is confirmed by the TEM images (not included) which show the absence of CuO particles, although the EDX analysis confirms the presence of elementary copper. By contrast, the Cu/SBA-f-500 material is characterized by the formation of copper oxide nanoparticles (Figure 1) whose size, as observed by TEM, is comprised between 5 and 10 nm. In fact, the XRD pattern at wide angles (Figure 1) reveals characteristic diffraction peaks ((-111), (002), (111), (200) and (-202)) of crystalline CuO. In line with the TEM observations, the large width of the peaks suggests a small crystallite size. The majority of these nanoparticles appear to be located in the channels of the SBA-15 mesoporous silica support. This hypothesis is supported by the delay observed on the desorption branch of the nitrous oxide physisorption isotherm, due to the partial plugging of the pores by the CuO particles. However, according to TEM, large sized copper particles (several hundreds of nanometers

5

to a few micrometers) are also present on the outside of the mesoporous channels. The significant differences between the Cu/SBA-r-500 and Cu/SBA-f-500 materials show the great impact of the calcination conditions on the dispersion of copper. Calcination with a temperature ramp promotes the formation of Cu-O-Si species, whereas flash calcination results in the predominant formation of well crystallized CuO nanoparticles confined in the channels of the mesoporous silica support.
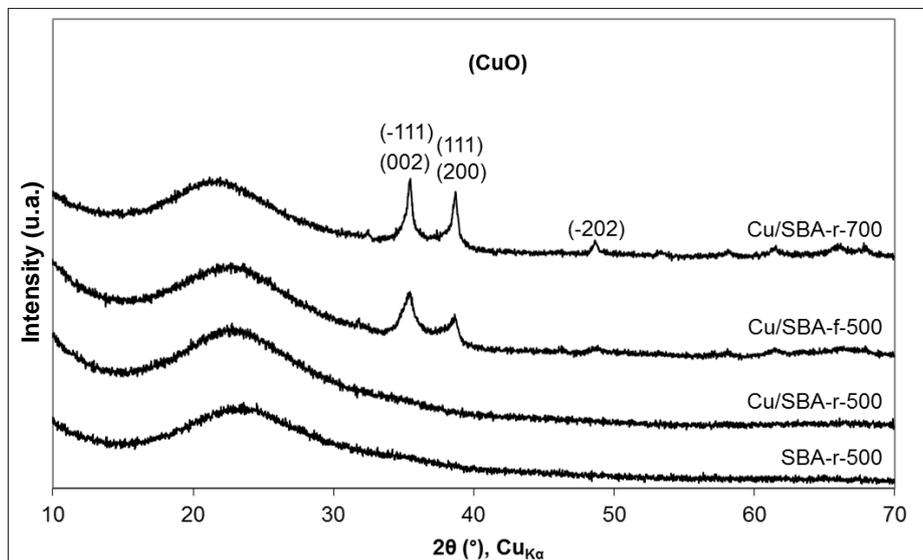

Figure 1: XRD patterns at wide angles of the SBA-r-500 support and the Cu/SBA-15 adsorbents obtained by solid-solid grinding.

Calcination at 700°C (Cu/SBA-r-700 material) results in the copper-based species being sintered into large sized CuO particles. Based on the TEM and SEM characterizations, it is difficult to quantify which particle population is predominant. However, the XR diffraction peaks of the CuO of the Cu/SBA-r-700 adsorbent (Figure 1), which are sharper than those of the Cu/SBA-f-500 material, suggest a larger average crystallite size for the material calcined at 700°C.

The SO_2 adsorption tests were performed in a fixed-bed reactor at 400°C with a gaseous mixture consisting of 250 ppm of SO_2 and 10 vol. % of oxygen in nitrous oxide. The SO_2 breakthrough curves obtained are shown in Figure 2.

The SO_2 adsorption capacity of these different adsorbents was measured. Since copper is present in different forms (Cu-O-Si species, nanoparticles and micrometric particles of CuO) in the adsorbents, the degree of sulfation of copper was calculated for each adsorbent and is considered as a representative value of the efficiency of the incorporated active phase (copper). The SO_2 adsorption capacities SO_2 (C_{ads}), obtained by integration of the SO_2 breakthrough curves up to the threshold value of 75 ppm and expressed in mol_{SO2}/g_{ads}, as well as the copper sulfation rate (TSC in %) are given in Table 1. The results show that a correlation exists between the dispersion of copper and the desulfurization efficiency of the adsorbent. The large size of the CuO particles of the adsorbent Cu/SBA-r-700 results in the low efficiency of the latter (C_{ads} = $1.7x10^{-5}$ mol_{SO2}/g_{ads}, TSC = 1.1%). In fact, according to the literature (9; 10), sulfation of the "core" of the CuO particles is very slow, in particular for large particles. Indeed, Centi *et al.* (9) suggest there is a rapid formation of a surface copper sulfate layer, which slows down the formation of the "core" sulfates. The small average size of

6

the CuO particles of the adsorbent Cu/SBA-f-500 allows a greater efficiency (C_{ads} = 1.3×10^{-4} mol_{SO2}/g_{ads}, TSC = 10.0%) to be obtained, due to the better dispersion of CuO. Finally, the Cu-O-Si species of the adsorbent Cu/SBA-r-500 are found to be much more efficient because the latter exhibits the best SO_2 adsorption capacity (C_{ads} = 4.5×10^{-4} mol_{SO2}/g_{ads}) and also the highest copper sulfation rate (TSC = 28.1%). The overall results therefore show that the efficiency of the adsorbent increases with the dispersion of copper and that the Cu-O-Si species are the most active for the desulfurization reaction.

Table 1: Copper contents, SO_2 adsorption capacities and degrees of sulfation of copper of the adsorbents obtained by solid-solid grinding.

Adsorbent	Cu/SBA-r-500	Cu/SBA-f-500	Cu/SBA-r-700
CuO (mol/g_{ads})	1.6×10^{-3}	1.3×10^{-3}	1.5×10^{-3}
C_{ads}^{a} (mol_{SO2}/g_{ads})	4.5×10^{-4}	1.3×10^{-4}	1.7×10^{-5}
Degree of sulfation of copper (TSC) (%)	28.1	10.0	1.1

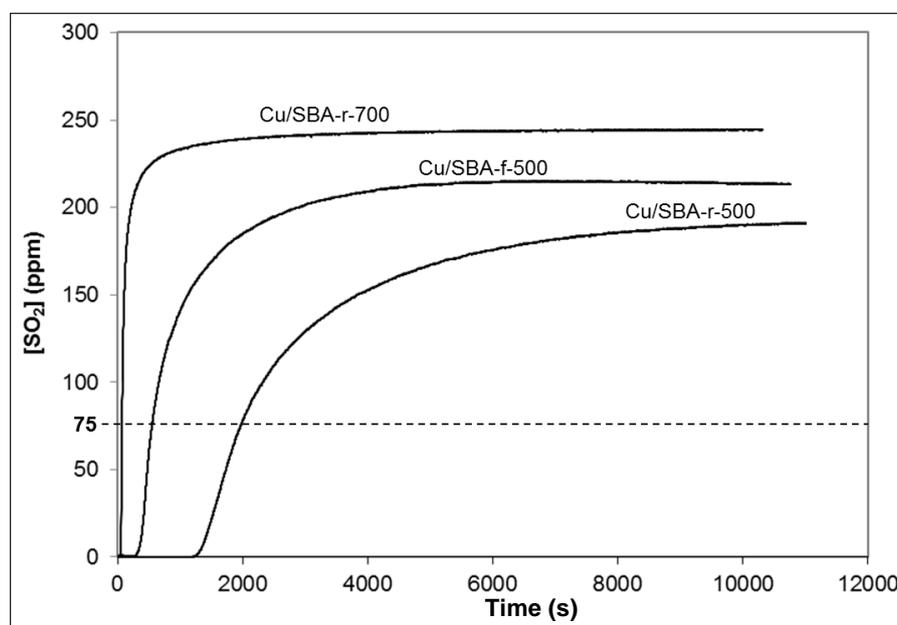^{a}Determined by integration of the breakthrough curves up to [SO_2] = 75 ppm.

Figure 2: SO_2 breakthrough curves of adsorbents obtained by solid-solid grinding.

Next, we studied the impact of the copper content on the behavior of the materials during successive adsorption-regeneration cycles (multi-cycle tests). The materials were prepared by wet impregnation of the copper nitrate. This method allows, while controlling the calcination conditions (calcination in fixed-bed reactor under high synthetic air flow), to obtain, in a simple and reproducible way, highly dispersed Cu-O-Si species on the SBA-15 mesoporous silica support (11; 12; 13; 14; 15). Three materials - $CuO_{8,8}$/SBA, $CuO_{15,6}$/SBA and $CuO_{31,7}$/SBA, with CuO contents of 8.8 wt. %, 15.6 wt. % and 31.7 wt. % respectively, were compared. The physicochemical characterizations confirm the preservation of the ordered mesoporous structure and the presence of (mostly) Cu-O-Si species for the three materials. The SO_2 adsorption capacities of the adsorbents as a function of the number of chemisorption-regeneration cycles are shown in Figure 3.
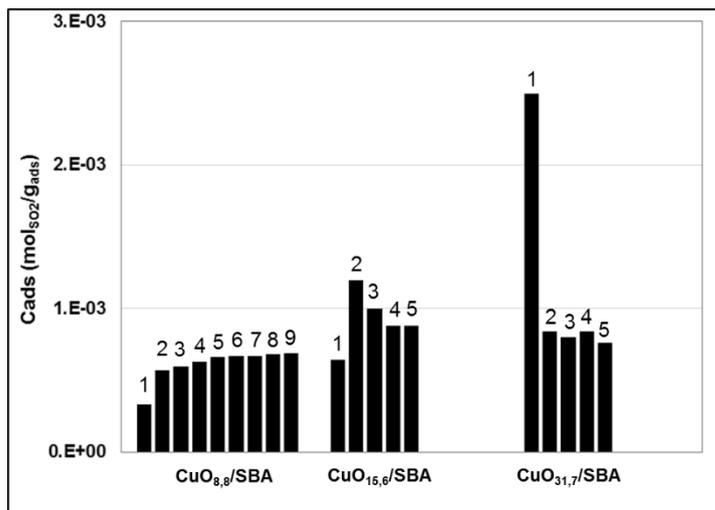
7

Figure 3 : SO_2 (C_{ads}) adsorption capacities of the adsorbents as a function of the number of chemisorption-regeneration cycles.

After the first chemisorption-regeneration cycle, the efficiency of the adsorbent $CuO_{8,8}$/SBA increases significantly. Indeed, the sulfation capacity is $C_{ads} = 3.3 \times 10^{-4}$ mol_{SO2}/g_{ads} (TSC = 29.7%) during the first cycle, and reaches $C_{ads} = 5.7 \times 10^{-4}$ mol_{SO2}/g_{ads} (TSC = 51.4%) during the second chemisorption. It was found that heat treatment at 600°C under N_2 (material regeneration treatment) is at the origin of the increase in efficiency of the adsorbent. According to the literature, it is possible that such a treatment results in the reduction of Cu^{2+} ions in Cu^+ species (16; 17) which may prove to be more active for the SO_2 oxidation-chemisorption reaction. After the second cycle, the capacity of the adsorbent continues to increase significantly until $C_{ads} = 6.9 \times 10^{-4}$ mol_{SO2}/g_{ads} during the 9th cycle (TSC = 62.2%). This absence of deactivation is due to the low copper content which prevents sintering of the copper. In fact, the characterizations of the adsorbent after 9 cycles suggest that most of the copper is still present in the form of Cu-O-Si.

Conversely, the $CuO_{31,7}$/SBA adsorbent exhibits a high adsorption capacity ($C_{ads} = 25.4 \times 10^{-4}$ mol_{SO2}/g_{ads} and TSC = 63.6%) during the first cycle, due to the high copper content of the adsorbent. The latter falls steeply from the second cycle ($C_{ads} = 8.4 \times 10^{-4}$ mol_{SO2}/g_{ads} and TSC = 21.1%) and continues to drop gradually until it reaches $C_{ads} = 7.6 \times 10^{-4}$ mol_{SO2}/g_{ads} and TSC = 19.0%, during the 5th cycle. This effect is due to the sintering of the copper-based species into larger sized copper oxide particles (CuO), as demonstrated by the characterizations of the adsorbent (not included) after 5 cycles. The chemisorption-regeneration tests suggest that the sintering of copper occurs predominantly from the 1st cycle for this absorbent. This demonstrates that the Cu-O-Si species are unstable for a too high copper content.

The $CuO_{15,6}$/SBA material exhibits an intermediate behavior between previous two materials ($CuO_{8,8}$/SBA and $CuO_{31,7}$/SBA). Indeed, when compared to the $CuO_{8,8}$/SBA adsorbent, we see a significant increase in efficiency between the 1st ($C_{ads} = 6.8 \times 10^{-4}$ mol_{SO2}/g_{ads} and TSC = 34.7%) and 2nd cycle ($C_{ads} = 12.0 \times 10^{-4}$ mol_{SO2}/g_{ads} and TSC = 61.2%). And similarly to the $CuO_{31.7}$/SBA material, a gradual deactivation of the adsorbent is observed between the 2nd and 5th cycle until $C_{ads} = 8.8 \times 10^{-4}$

8

mol_{SO2}/g_{ads} and TSC = 44.9% during the 5th cycle. The physicochemical characterizations of the adsorbent after 5 cycles show that a portion of the copper-based species sinter and may give rise to larger sized CuO particles, but to a lesser extent than in the case with the $CuO_{31.7}$/SBA material.

All the physicochemical characterizations of the $CuO_{8,8}$/SBA, $CuO_{15,6}$/SBA and $CuO_{31,7}$/SBA adsorbents after the last chemisorption-regeneration cycle demonstrate that the textural properties of the adsorbents are partially altered (reduction of BET surface areas and porous volumes). This effect is probably connected with the sintering of the copper-based species into CuO particles (i. e. increase in the fraction of core CuO). It seems that the higher the copper content, the more important this phenomenon becomes. The efficiency of the copper for the desulfurization reaction is reduced to the same extent.

With a too low content, the efficiency of the adsorbent remains stable during the chemisorption-regeneration cycles due to the stability of the Cu-O-Si species, but seems to be limited by the low copper content. With a too high content, there is substantial sintering of the copper-based species into larger sized CuO particles, from the 1st cycle, leading to a significant loss of efficiency of the adsorbent for the next cycles. The highest SO_2 adsorption capacity after 5 cycles is obtained for the $CuO_{15.6}$/SBA adsorbent $CuO_{15,6}$/SBA (C_{ads} = 8.8x10^{-4} mol_{SO2}/g_{ads} and TSC = 44.9%). These results show that there is an optimal CuO content, beyond which the sintering of the copper-based species into CuO particles results in a significant reduction in efficiency of copper during desulfurization, under the conditions used during the adsorption/regeneration tests.

4. Conclusions

All the work carried out under the DeSO$_X$ New Gen program demonstrates that:

- The SBA-15 mesoporous silica selected as support is inert to SO$_X$ (no sulfation of the support), exhibits good thermal stability, and has a pore size that allows for easy diffusion of the SOx in the mesoporous network.
- The copper oxide alone supported on SBA-15 mesoporous silica is active for the oxidation of SO_2 to SO_3, readily chemisorbs the SOx in the form of sulfates, and the decomposition temperature of the latter (~ 700°C) allows us to consider the development of a regenerable adsorbent.
- Depending on the synthesis conditions for the CuO/SBA-15 type adsorbents, it is possible to obtain different copper-based species: CuO particles of micrometric size, CuO nanoparticles (5 to 10 nm) and highly dispersed Cu^{2+} species strongly interacting with the support (Cu-O-Si).
- The Cu-O-Si species are the most efficient for the desulfurization reaction.
- The heat treatment at 600°C under a nitrogen flow allows the efficiency of the adsorbents to be increased significantly. This effect may be connected with the formation of Cu^+, demonstrated by XPS (spectra not included).
- The multi-cycle studies demonstrated that the textural properties of the SBA-15 support are partially affected during the chemisorption-regeneration cycles and that the moderate deactivation of the adsorbents is due primarily to the sintering of the copper-based species and the partial alteration of the SBA-15 mesoporous silica support.

9

- An optimal copper content exists for the efficiency of the adsorbent. A too low copper content results in a stable material that prevents sintering of copper, but that is less efficient during desulfurization. A too high copper content results in a less stable material without any significant gain in efficiency, due to the substantial sintering of copper oxide after a few operating cycles, under the conditions used during this study.

5. Bibliography

1. *Adsorption of SOx by oxide materials: A review.* **Y. Mathieu, L. Tzanis, M. Soulard, J. Patarin, M. Vierling, M. Moliere.** 2013, Fuel Processing Technology, Vol. 114, pp. 81–100.

2. *Rapid functionalization of mesoporous materials: directly dispersing metal oxides into as-prepared SBA-15 occluded with template.* **Y. M. Wang, Z. Y. Wu, L. Y. Shi, J. H. Zhu.** 2005, Advanced Materials, Vol. 17, pp. 323-327.

3. *Adsorptive Desulfurization by Copper Species within Confined Space.* **W-H. Tian, L-B. Sun , X-L. Song, X-Q. Liu, Y. Yin, G.-S. He.** 2010, Langmuir, Vol. 26, pp. 17398–17404.

4. *Surface functionalization of SBA-15 by the solvent-free method .* **Y. M. Wang, Z. Y. Wu, J. H. Zhu.** 2004, Journal of Solid State Chemistry, Vol. 177, pp. 3815–3823.

5. *Influence of silica and alumina supports on the temperature-programmed reduction of copper(II) oxide.* **S. J. Gentry, P. T. Walsh.** 1982, J. Chem. Soc. Faraday. Trans. 1, Vol. 78, pp. 1515-1523.

6. *Effect of Surface Acidity of CuO-SBA-15 on Adsorptive Desulfurization of Fuel Oils.* **X-C. Shao, L-H. Duan, Y-Y. Wu, X-C. Qin, W-G. Yu, Y. Wang, H-L. Li, Z-L. Sun, L-J. Song.** 2012, Acta Phys. -Chim. Sin., Vol. 28, pp. 1467-1473.

7. *CuO nanoparticles encapsuled inside Al-MCM-41 mesoporous materials via direct synthetic route.* **C. Huo, J. Ouyang.** 2013, Scientific Reports, Vol. 4, p. 3682.

8. *Investigation of the structure of MCM-41 samples with a high copper content.* **Y. Kong, H. Zhu, G. Yang, X. Guo, W. Hou, Q. Yan, M. Gu, C. Hu.** 8, 2004, Advanced Functional Materials, Vol. 14, pp. 816-820.

9. *Combined DeSOx/DeNOx reactions on a copper on alumina sorbent-catalyst. 1. Mechanism of SO_2 oxidation-adsorption.* **G. Centi, N. Passarini, S. Perathoner, A. Riva.** 1992, Ind. Eng. Chem. Res., Vol. 31, pp. 1947-1955.

10. *The preparation of supported NiO and Co_3O_4 Nanoparticules by the nitric oxide controlled thermal decomposition of nitrates.* **J. R. A. Sietsma, J. D. Meeldijk, J. P. den Breejen, M. Versluijs-Helder, A. Jos van Dillen, P. E. de Jongh, K. P. de Jong.** 2007, Angewandte Chemie International Edition, Vol. 46, pp. 4547-4549.

11. *Control of metal dispersion and structure by changes in the solid-state chemistry of supported cobalt Fischer–Tropsch catalysts.* **S. L. Soled, E. Iglesia, R. A. Fiato, J. E. Baumgartner, H. Vroman, S. Miseo.** 2003, Topics in Catalysis, Vol. 26, pp. 101-109.

12. *Copper Nitrate Redispersion To Arrive at Highly Active Silica-Supported Copper Catalysts.* **P. Munnik, M. Wolters, A. Gabrielsson, S. D Pollington, G. Headdock, J. H. Bitter, P. E. de Jongh,**

K. P. de Jong *. 2011, Journal of Physical Chemistry C, Vol. 115, pp. 14698–14706.

13. *The role of the 'glow phenomenon' in the preparation of sulfated zirconia catalysts.* **A. Hahn, T. Ressler, R. E. Jentoft, F. C. Jentoft.** 2001, Chemical Communication, pp. 537–538.

14. *Impact of Calcination Conditions on the Structure of Alumina-Supported Nickel Particles.* **B. Vos, E. Poels, A. Bliek.** 2001, Journal of Catalysis, Vol. 198, pp. 77–88.

15. *Container effect in nanocasting synthesis of mesoporous metal oxides.* **X. Sun, Y. Shi, P. Zhang, C. Zheng, X. Zheng, F. Zhang, Y. Zhang, N. Guan, D. Zhao, G. D. Stucky.** 2011, J. Am. Chem. Soc, Vol. 133, pp. 14542–14545.

16. *Autoreduction of Copper on Silica and Iron-Functionalized Silica Nanoparticles with Interparticle Mesoporosity.* **M. Popova, A. Ristic, M. Mazaj, D. Maucec, M. Dimitrov, N. Novak Tusar.** 2014, ChemCatChem, Vol. 6, pp. 271 – 277.

17. *Electron Paramagnetic Resonance Studies of Copper Ion-Exchanged ZSM-5 .* **S. C. Larsen, A. Aylor, A. T. Bell, J. A. Reimer.** 1994, J. Phys. Chem., Vol. 980, pp. 11533–11540.

The French Environment and Energy Management Energy (ADEME) participates in the implementation of public policies in the fields of the environment, energy, and sustainable development. The Agency offers its expertise and advisory capabilities to businesses, local governments, public administrations and the general public to enable them to make progress in their environmental efforts. In addition, it co-funds projects, from research to implementation, in the following fields: waste management, soil preservation, energy efficiency and renewable energies, air quality and noise control.

ADEME is a public agency under the joint supervision of the French Ministries for Ecology, Sustainable Development and Energy, and for National Education, Higher Education and Research.

Liberté • Égalité • Fraternité
RÉPUBLIQUE FRANÇAISE

MINISTÈRE
DE L'ÉCOLOGIE,
DU DÉVELOPPEMENT DURABLE
ET DE L'ÉNERGIE

MINISTÈRE
DE L'ÉDUCATION NATIONALE
DE L'ENSEIGNEMENT SUPÉRIEUR
ET DE LA RECHERCHE

ADEME
20, avenue du Grésillé
BP 90406 I 49004 Angers Cedex 01

www.ademe.fr